CHEMISTRY OF MATERIALS
Article

*Chem. Mater.* **2010,** *22,* 5411–5419 5411
DOI:10.1021/cm100090e

# Ordered Arrays of Nanorods Obtained by Solid−Liquid Reactions of LaOCl Crystals

P. Afanasiev,*,† M. Aouine,† C. Deranlot,† and T. Epicier‡

†*Institut de Recherches sur la Catalyse et l'environnement, CNRS-Université de Lyon-1, 2, av. A. Einstein, 69626, Villeurbanne Cedex, France, and* ‡*MATEIS, UMR CNRS 5510 Bat. B. Pascal, INSA de Lyon, 69626 Villeurbanne Cedex, France*

*Received January 11, 2010. Revised Manuscript Received August 12, 2010*

A new top−bottom approach is developed to prepare ordered arrays of nanorods, based on controlled etching, as exemplified by the case of LaOCl crystals. Molten-salt issued LaOCl was applied as a precursor, with highly anisotropic crystals oriented along the [001] axis. These LaOCl flat crystals are reactive toward aqueous solutions at room temperature, yielding ordered assemblies of rod-like crystals. Depending on the reaction mixture composition, nanorods of LaOCl itself or other La compounds can be obtained. The morphology of the products obtained in the solutions can be finely controlled by adding extraneous chemical species which modify the etching kinetics. Thus, LaOCl reacts with the acidic phosphate solutions, leading to the arrays of $LaPO_4$ nanorods, oriented along the [001] axis of the initial solid. By contrast, reaction with aqueous HCl produced assemblies of perpendicular rods, oriented along the [100] and [010] axes. The catalytic properties of the nanorods as obtained were tested in the decomposition of isopropanol. Strong differences of acid−base properties of differently oriented LaOCl particles have been observed.

## 1. Introduction

Morphology is a key property of materials, crucial for various applications. Tailor-made syntheses of uniformly sized nanoparticles have attracted great attention in the recent years.[1] Various oxides, metals and other inorganic materials have been prepared in quasi one-dimensional crystals.[2] Ordered nanostructures are of particular interest, in which the crystals are aligned in the same direction.[3−5] Besides mechanical and electro-optical applications, such objects represent a great interest for catalysis since tailor-made synthesis of solids with preferential orientation of crystallographic planes would allow fine control of the catalytic properties. Originally, lithography techniques have been applied to produce such structures.[6,7] Giving highly reproducible results, these techniques, however, are mostly not scalable and require expensive preparation procedures. Therefore, alternative methods were developed to obtain such ordered solids, in which the particles are usually formed by nucleation and growth from homogeneous solutions[8,9] or are grown on some ordered templates by means of some chemical, eletcrochemical, or physical process.[10−12] In this work, we demonstrate that the arrays of nanorods can be obtained from the process of solid−liquid reaction of an appropriate solid precursor. The structure of such arrays may be controlled by means of variation of the medium's reactivity and/or by the addition of specifically absorbing species.

The layered LaOCl compound was chosen for the case study. Lanthanide compounds such as oxides, sulfides, and phosphates have received much attention because of their unique optical and magnetic properties.[13−15] LaOCl is an inorganic material with a wide scope of applications ranging from catalysis[16−18] to luminescent materials, ion conductors, and sensors.[19−21] Preparation of this material in a controlled manner represents a challenge and is

*To whom correspondence should be addressed. E-mail: pavel.afanasiev@ircelyon.univ-lyon1.fr.

(1) Jain, P. K.; Huang, X.; El-Sayed, I. H.; El-Sayed, M. A. *Acc. Chem. Res.* **2008**, *41*, 1578.
(2) Morariu, M.; Voicu, N.; Schäffer, E.; Lin, Z.; Russell, T. P.; Steiner, U. *Nat. Mater.* **2003**, *2*, 48.
(3) Ji, Y. L.; Guo, L.; Xu, H.; Simon, P.; Wu, Z. *J. Am. Chem. Soc.* **2002**, *124*, 14864.
(4) Vayssieres, L.; Rabenberg, L.; Manthiram, A. *Nano Lett.* **2002**, *2*, 1393.
(5) Xi, J.-Q.; Kim, J. K.; Schubert, E. F. *Nano Lett.* **2005**, *5*, 1385.
(6) Burmeister, F.; Badowsky, W.; Braun, T.; Wieprich, S.; Boneberg, J.; Leiderer, P. *Appl. Surf. Sci.* **1999**, *144*, 461.
(7) Boto, A. N.; Kok, P.; Abrams, D. S.; Braunstein, S. L.; Williams, C. P.; Dowling, J. P. *Phys. Rev. Lett.* **2000**, *85*, 2733.
(8) Peng, P.; Liu, X. D.; Sun, C. S.; Ma, J. M.; Zheng, W. J. *J. Solid State Chem.* **2009**, *182*, 1003.
(9) Tian, Z. R.; Voigt, J. A.; Liu, J.; Mckenzie, B.; Mcdermott, M. J.; Rodriguez, M. A.; Konishi, H.; Xu, H. *Nat. Mater.* **2003**, *2*, 821.
(10) Xu, L.; Liao, Q.; Zhang, J.; Ai, X.; Xu, D. *J. Phys. Chem. C* **2007**, *111*, 4549.
(11) Xia, F.; Brugger, J.; Ngothai, Y.; O'Neill, B.; Chen, G.; Pring, A. *Cryst. Growth Des.* **2009**, *9*, 4902.
(12) Hu, Z. A.; Wu, H.; Shang, X.; Lü, R. J.; Li, H. L. *Mater. Res. Bull.* **2006**, *41*, 1045.
(13) Stouwdam, J. W.; Raudsepp, M.; van Veggel, F. C. J. M. *Langmuir* **2005**, *21*, 7003.
(14) Cao, Y. C. *J. Am. Chem. Soc.* **2004**, *126*, 7456.
(15) Lehmann, O.; Kömpe, K.; Haase, M. *J. Am. Chem. Soc.* **2004**, *126*, 14935.
(16) Peringer, E.; Salzinger, M.; Hutt, M.; Lemonidou, A. A..; Lercher, J. A. *Top. Catal.* **2009**, *52*, 1220.
(17) Au, C. T.; He, H.; Lai, S. Y.; Ng, C. F. *Appl. Catal., A* **1997**, *159*, 133.
(18) Podkolzin, S. G.; Stangland, E. E.; Jones, M. E.; Peringer, E.; Lercher, J. A. *J. Am. Chem. Soc.* **2007**, *129*, 2569.


Published on Web 09/07/2010

actively pursued. Thus, recently a synthesis of uniformly sized and ultrathin LaOCl nanoplates was reported via the thermolysis of a trichloroacetate precursor in long chain amine and 1-octadecene.[22] Nanofibers of LaOCl were obtained from the PVA lanthanum chloride composites.[23] In the present work, we describe the preparation of highly anisotropic crystals of LaOCl using molten salt synthesis and then report on their reactivity toward aqueous solutions, which results in the ordered arrays of nanorods of different crystallographic orientation. Then we demonstrate that the formation of nanorods from the flat crystals is accompanied with a drastic change of the catalytic properties.

## 2. Experimental Section

To obtain the LaOCl solid, hydrated $LaCl_3$ from Aldrich and a 5−10-fold molar excess of $LiNO_3$ were thoroughly mixed and placed in a Pyrex reactor. The mixtures were pretreated under nitrogen flow at 150 °C for 2 h, then the reaction was carried out at 400−550 °C for 4 h. After cooling, the solidified melt was washed with distilled water at room temperature, and then the product was separated and dried overnight in air at 100 °C. Solution reactions of LaOCl were carried out at ambient temperature. In typical syntheses, a weighted amount of ca. 0.2 g of LaOCl was stirred for 30 min with 10 mL of 0.02 M HCl or with a large excess of 0.1 M acidic ammonium phosphate salt ($NH_4H_2PO_4$, at its own pH).

XRD patterns were recorded on a Bruker diffractometer by using CuKα radiation. Identification of phases was made using standard JCPDS files. Surface areas and pore radii distributions were measured by nitrogen adsorption. Chemical analyses of alkali metals and titanium were carried out by using the atomic emission method.

Scanning electron microscopy (SEM) images were obtained on a Hitachi S800 device, at Center of Electronic Microscopy, Claude Bernard University (Lyon-1). Transmission electron micrographs were obtained on a JEOL 2010 device with an accelerating voltage 200 KeV. AFM images were obtained with a NanoScope III Multimode (Digitial Instruments) microscope operated in air at room temperature. To obtain a representative analysis of the surface, local areas (~10 $\mu$m × 10 $\mu$m) separated by ~1 mm were inspected. Images are shown in top-view scale representation (dark color corresponds to minima).

The Raman spectra of samples were recorded with a UV−vis−NIR LabRam HR Raman spectrometer (Horiba−Jobin Yvon) equipped with a confocal microscope, Notch filter, and CCD detector. The diffused light was spatially dispersed with 1800 grooves/mm or 300 grooves/mm diffraction grating. A long working distance objective (×50) allowed for the focusing of a laser and the collection of retro-diffused light in the cells. The laser power on the samples was typically 2 mW, conditions under which no significant laser heating was observed. The violet exciting line at 458 nm of a 2018 RM $Ar^+$−$Kr^+$ laser (Spectra physics) was applied.

The XPS spectra were recorded on an Axis Ultra DLD device (Kratos Analytical). The samples were pressed on an indium foil attached to the sample holder and transported into the preparation chamber of the XPS machine. The sample excitation was done by Al K X-rays (1486.6 eV). Peak shifts due to the charging of the samples were corrected by taking the C 1s line of carbon residuals at 285.0 eV as a reference. Quantitative analysis was carried out using the device-attached software. Thermodynamic parameters of the solid−liquid reactions were calculated using the HSC Chemistry program (Outotec Research Oy).

Catalytic activities were measured for isopropanol (IPA) decomposition at atmospheric pressure in a fixed-bed flow microreactor. Prior to catalytic tests, all of the solids were preheated in nitrogen flow at 300 °C for 1 h, to desorb the impurities coming from ambient air. In the chosen temperature range, 250−350 °C, the IPA conversion was adjusted to be below 20% under the conditions used (100 mL/min gas flow, 50−100 mg of catalyst), and the plug−flow reactor model was used to calculate the specific reaction rate according to the equation $Vs = -(F/m)\ln(1 - x)$, where $F$ is the IPA molar flow (mol/s), $m$ is the catalyst mass (g), and $x$ is the conversion. Acetone and propene formation rate constants and activation energies were measured in order to compare the acid−base properties of the solids. The products were analyzed chromatographically. Steady state activities were compared after 16 h of on stream tests.

## 3. Results and Discussion

**3.1. Preparation and Properties of the LaOCl Thin Plate Crystals.** Molten salts as reaction media provide an alternative to aqueous chemistry for materials synthesis, due to altering the solubility and/or the reactivity of species.[24−26] Molten nitrates can react as oxobases, i.e., donate oxygen ions to appropriate oxoacids. Because of this property, precipitation of different oxides, oxosalts,[27] and more complex structures, such as sodalites,[28] is possible in these ionic solvents. For the lanthanum chloride precursor, the following reactions are possible, leading to the La(III) oxide as a final product.

$$LaCl_3 + 2LiNO_3 \rightarrow LaOCl + 2LiCl + 2NO_2 + 1/2O_2 \quad (1)$$

$$2LaOCl + 2LiNO_3 \rightarrow La_2O_3 + 2LiCl + 2NO_2 + 1/2O_2 \quad (2)$$

However, due to the relatively low oxoacidity of the La(III) ions, their reactivity in the molten nitrates is low, and reaction 2 is difficult, and only reaction 1 occurs at 450−500 °C. Therefore, pure LaOCl was obtained with quantitative yield. Its identity has been confirmed by XRD and chemical analysis. Elemental analysis showed a good agreement with LaOCl stochiometry, and the absence of alkali metal impurities (Table S1 of Supporting Information).

(19) Marsal, A.; Centeno, M. A.; Odriozola, J. A.; Cornet, A.; Morante, J. R. *Sens. Actuat. B* **2005**, *108*, 484.
(20) Okamoto, K.; Imanaka, N.; Adachi, G. *Solid State Ionics* **2002**, *154−155*, 577.
(21) Marchal, A.; Rossinyol, E.; Bimbela, F.; Tellez, C.; Coronas, J.; Cornet, A.; Morante, J. R. *Sens. Actuat. B* **2005**, *109*, 38.
(22) Du, Y. P.; Zhang, Y. W.; Sun, L. D.; Yan, C. H. *J. Am. Chem. Soc.* **2009**, *131*, 3162.
(23) Chen, Y.; Qian, Q.; Liu, X.; Xiao, L.; Chen, Q. *Mater. Lett.* **2010**, *64*, 6.
(24) Afanasiev, P.; Geantet, C. *Coord. Chem. Rev.* **1998**, *178−180*, 1725.
(25) Afanasiev, P. *Mater. Lett.* **1998**, *34*, 253.
(26) Afanasiev, P. *Mater. Lett.* **2007**, *61*, 4622.
(27) Afanasiev, P. *Chem. Mater.* **1999**, *11*, 1999.
(28) Afanasiev, P. *Chem. Mater.* **2001**, *13*, 459.

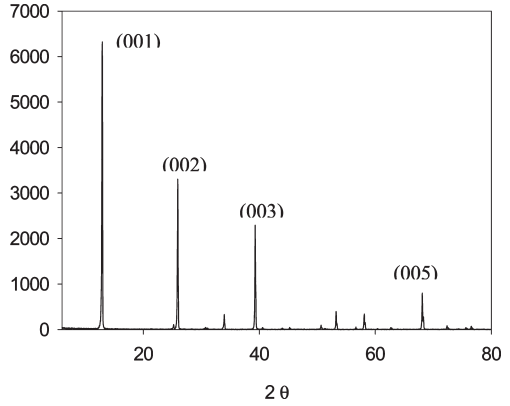


**Figure 1.** XRD pattern of LaOCl obtained in molten $LiNO_3$ at 773 K. All peaks correspond to the LaOCl phase; the marks are the Miller indices of selected planes.

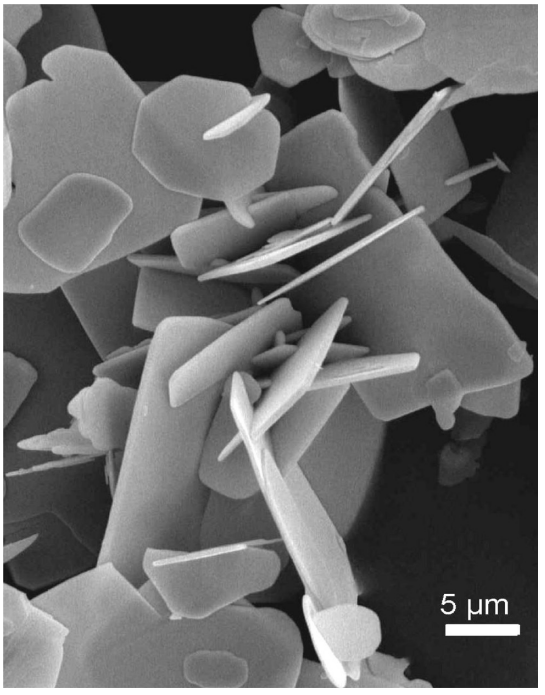


**Figure 2.** SEM image of the initial LaOCl crystals at magnification ×6000.

The LaOCl solid as prepared possessed highly oriented plate-like morphology (Figure 1). SEM images showed thin sheets of 5−20 $\mu$m size with rectangular or truncated rectangular shape. The thickness of the crystals was at the nanometric scale and were therefore impossible to determine from SEM. The XRD patterns showed a pure LaOCl phase with strongly enhanced intensity for the {00n} lines and virtual disappearance of any other reflexes (Figure 2), as compared to the JCPDS reference pattern (JCPDS 01-08-0064). Because of the extreme shape anisotropy effect, the peak of the (005) reflection was observed, which is not listed in the JCPDS file. High resolution HAADF of LaOCl crystallites showed atomic columns arranged along the [001] axis, proving very high ordering in this material (Figure 3). Low magnification and diffraction contrast transmission microscopy showed perfect $C_4$ symmetry Kikuchi patterns (or complementary bending lines in real space)

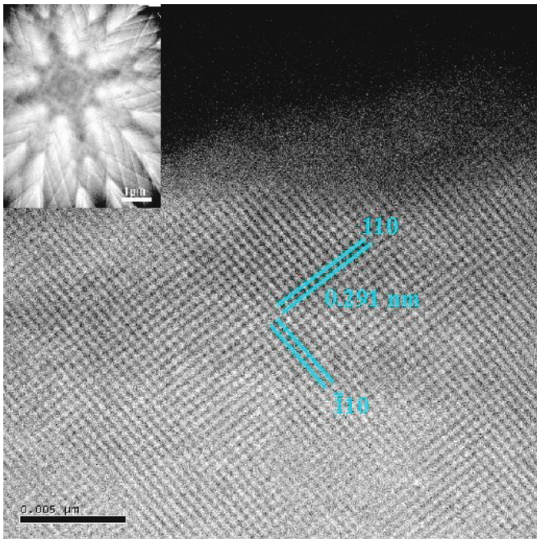


**Figure 3.** HAADF image of a LaOCl crystallite viewed along the [001] axis. The scale bar length is 5 nm. Insert: Kikuchi patters at magnification ×8000.

with similar intensities of lines from the same families (Figure 3, insert). This indicated a perfect [001] orientation of particles and high uniformity of the crystallite's thickness. EDS analysis revealed the high homogeneity of composition within the limits of accuracy of this method (Figure S1 of Supporting Information).

The particular morphology observed for LaOCl prepared in molten nitrate can be explained by the properties of the preparation medium. Being completely ionized solvents, molten salts show strong selectivity of solvation toward differently charged crystalline planes of the solids. The solids having the structures containing low-index charged planes often yield anisotropic morphologies when being grown in the nitrate fluxes.[29] This is certainly the case with LaOCl, which has a lamellar structure with charged (001) planes.[30] Obviously, the growth rate along the neutral and therefore less solvated (100) and (010) planes should be much greater than along the charged chloride-populated (001) planes, which are probably strongly solvated by alkali metal ions.

Initially, we intended to use the obtained LaOCl as a precursor for obtaining new compounds by solid−gas reactions or by metathesis as recently described in ref 31. Indeed, such reactions (e.g., with $H_2S$ or $NH_3$) can occur, leading to some interesting products, which will be described elsewhere. However, we observed that even at room temperature upon a contact with some aqueous solutions LaOCl undergoes deep transformations. Either the initial LaOCl preserved its chemical identity but undergoes drastic changes of morphology, or it formed new nanocystalline phases, as follows.

**3.2. Etching with Acids and Bases.** Reaction with the excess of 0.1 M HCl after 4 h of contact led to the complete dissolution of LaOCl with the formation of

(29) Afanasiev, P. *J. Mater. Sci.* **2006**, *41*, 1187.
(30) Templeton, D. H.; Dauben, C. H. *J. Am. Chem. Soc.* **1953**, *75*, 6069.
(31) Charkin, D. O.; Grischenko, R. O.; Sadybekov, A. A.; Goff, R. J.; Lightfoot, P. *Inorg. Chem.* **2008**, *47*, 3065.

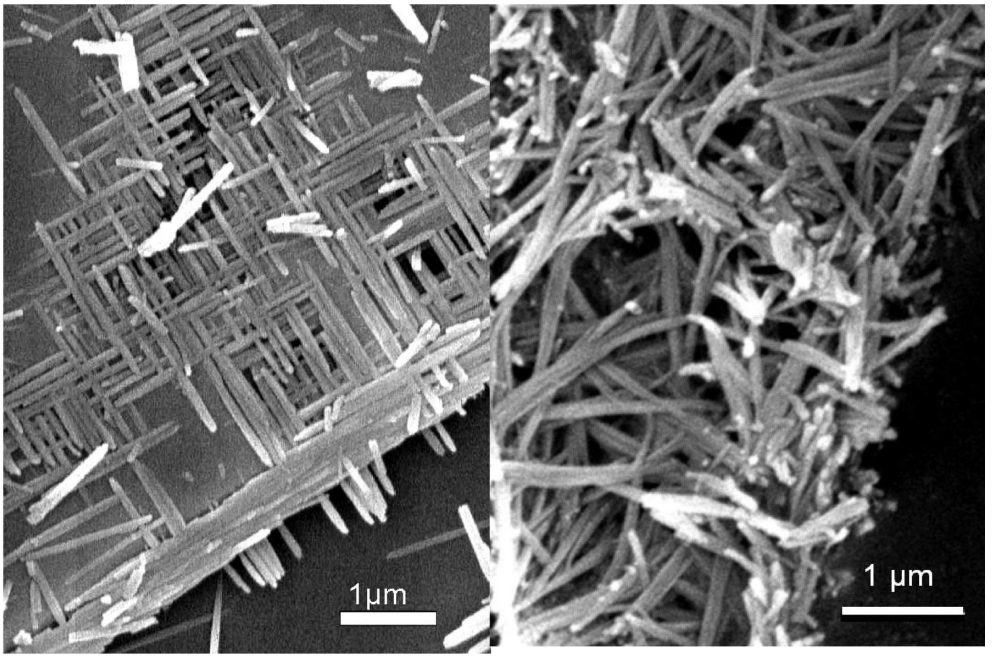


**Figure 4.** Arrays of perpendicularly oriented LaOCl rods, obtained by the etching of LaOCl with 0.05 M HCl for 0.5 h (a) and fibrous particles of $La(OH)_3$ obtained from the reaction with neutral water for 2 days (b).

transparent solutions, presumably according to the following reaction:

$$LaOCl + 2H^+ \rightarrow La^{3+} + Cl^- + H_2O \qquad (3)$$

If, however, 0.05 M diluted HCl solution was applied for 0.5 h, the dissolution was only partial, and the XRD pattern of the solid product corresponded to pure LaOCl. Energy dispersive X-ray spectroscopy (EDS) analysis revealed the presence of La, Cl, and O with an atomic ratio close to 1:1:1. SEM observations showed that the morphology was strongly changed. The arrays of perpendicularly crossed rods were observed (Figure 4a). It follows from SEM data that the reaction front propagates along the (100) and (010) directions. Because of the tetragonal symmetry of the LaOCl structure, the solid reactivity must be the same along these directions. As a result, arrays of perpendicularly oriented rods were obtained. At the same time, the specific surface area of the solid increased from 6 to 28 $m^2/g$, in agreement with the observed destruction of the LaOCl layers. The TEM study showed that at the initial stage of etching (5 min of stirring in the solution), rectangular voids are formed, propagating from the border into the solid along the [100] and [010] directions (Figure 5a). Lower magnification bright field diffraction contrast images showed the formation of perpendicularly crossed defects (Figure 5b). AFM images show slight roughness of the surface of the acid-treated sample at the scale of several nanometers (Figure 6a). At the same time, terraces of variable thickness from 20 to 100 nm were observed (Figure 6b). Therefore, the relative part of the (100) and (010) planes in the solid increased by an order of magnitude in the acid-etched solid.

According to XPS data, because of the increase of (110) and (010) planes exposure, the surface composition slightly changes. In the initial solids, the La to Cl ratio of 1.05 is closer to stoichiometric value, but after etching, the amount of chlorine on the surface decreased, and the La/Cl atomic ratio increases to 1.12 (Table S2 of Supporting Information). Note that no strong difference between surface compositions and the results of elemental analysis were observed, indicating that the material reacts as a whole and not only on the surface.

When more diluted acid (or neutral water) was applied, at pH 3 and higher, the solid was quantitatively transformed to fibrous lanthanum hydroxide ($La(OH)_3$). The obtained hydroxide had a specific surface area between 30 and 50 $m^2/g$ depending on the pH of reaction medium. Unlike the straight and perpendicularly aligned LaOCl rods, the $La(OH)_3$ particles are disordered and bent (Figure 4b). The sizes of LaOCl rods and $La(OH)_3$ are similar, which makes us suppose that there are some common steps in their formation. It seems that the same mechanism of etching perpendicularly to the [001] axis underlies both formations of the LaOCl and $La(OH)_3$ nanorods. Probably the destruction of LaOCl layers to form the rods occurs first, and depending on pH, then they can be further hydrolyzed to form $La(OH)_3$. This last hydrolysis step is accompanied by bending and disordering of solid particles. If, however, the pH is lower than some critical value near 2, the solid lanthanum hydroxide cannot be formed, being immediately dissolved. The increase of the lanthanum oxide species' solubility with a lowering of pH is quite expected and has been documented previously.[32]

(32) Yorukoglu, A; Girgin, I. *Hydrometallurgy* **2001**, *61*, 185.

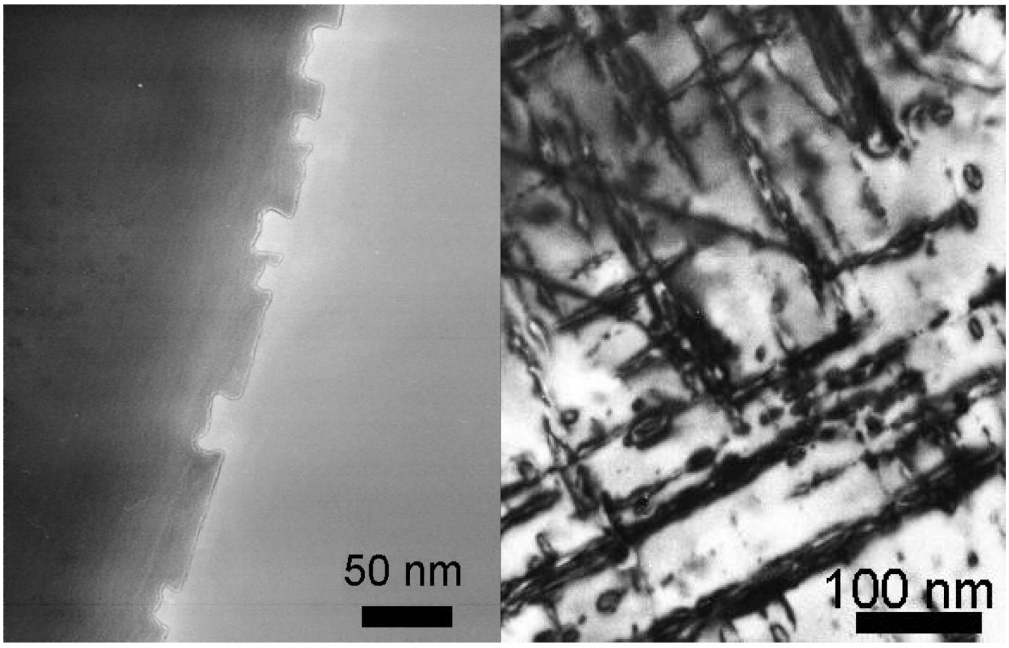


**Figure 5.** Rectangular cavities on the edge of LaOCl treated for 5 min with 0.02 M HCl (a) and the bright field image of perpendicularly oriented defects in the same sample (b).

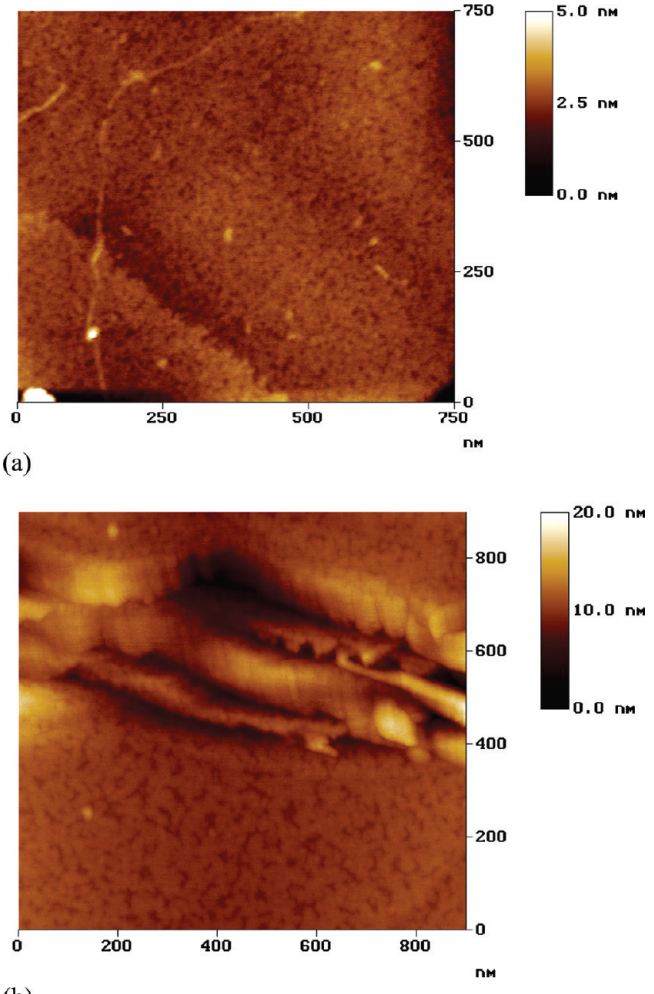


**Figure 6.** AFM images of LaOCl treated with 0.05 M HCl for 0.5 h, perpendicular to the [001] axis (a) and at some intermediate angle to it (b).

Recently, transformation of hydrothermally prepared LaOCl to $La(OH)_3$ nanorods was reported in neutral water and in the diluted acidic and basic solutions, in the pH range from 3 to 10.[33] Our results are in good agreement with this work within the same pH range, but strongly differ from it at lower and higher pH values outside of this range. Worth noting with this respect, that the equilibrium of reaction 4 (Table S3 of Supporting Information) should be shifted to the left by decreasing pH.

$$LaOCl + 2H_2O \rightarrow La(OH)_3 + HCl \qquad (4)$$

Note also that the formation of LaOCl nanorods due to etching with HCl is an essentially nonequilibrium phenomenon. Indeed, dissolution of LaOCl and $La(OH)_3$ in hydrochloric acid are favorable processes in the whole range of acidic pH (Tables S4 and S5 of Supporting Information).

Upon the increase of pH toward the basic region, one can expect an easy hydrolysis toward the hydroxide (Table S6 of Supporting Information). Surprisingly, treatment with an excess of 0.02 or 0.1 M KOH for 24 h did not lead to any measurable change in the amount of solid, nor in the phase composition. Only some decrease of the {00n} line intensity was noted. TEM observations showed that the flat crystallites remained intact. However, bright field low resolution TEM showed an increased frequency of bending lines along the sheets, suggesting that the crystals are somewhat deformed after contact with KOH. However, no potassium was found in the KOH-treated solid by EDS. Again, in a seeming disagreement with the results by Lee and Byeon,[33] plate-like LaOCl was not transformed to hydroxide in basic solutions. This difference might be explained by the particular morphology of the

(33) Lee, S. S.; Byeon, S. H. *Mater. Sci. Eng, B.* **2006**, *133*, 77.

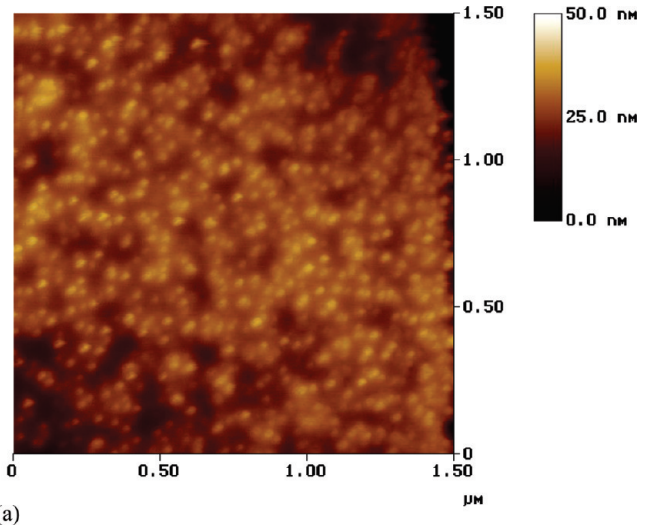


(a)

**Figure 7.** AFM image of the LaOCl surface treated with ammonium dihydrogen phosphate after 10 min of reaction.

solid under study. It exposes almost exclusively basal (001) planes, which should be negatively charged at high pH and therefore not be reactive toward the basic solutions. By this reason the following reaction, though being thermodynamically favorable, cannot proceed to a significant degree at pH values higher than 10.

$$LaOCl + OH^- + H_2O \rightarrow La(OH)_3 + Cl^- \qquad (5)$$

**3.3. Reaction with Acidic Ammonium Phosphate.** The reactivity of LaOCl was further studied toward three differently substituted ammonium phosphates at various concentrations. While tribasic and dibasic salts did not react, dihydrogen ammonium phosphate $(NH_4)H_2PO_4$ rapidly induced a deep transformation of the solid. According to AFM, already after 15 min of reaction in the 1 M phosphate solution, the surface of LaOCl became uneven, covered with the grains of mean size 30 nm, i.e., similar to the size of the nanorods obtained after 100 h of reaction (Figure 7). We see therefore that from the very beginning of the reaction, different crystalline planes are involved, as compared with acid etching.

After treating LaOCl with acidic phosphate, the $LaPO_4$ phase (JCPDS 01−075−1881) was detected in the XRD patterns. Therefore, the metathesis reaction occurred according to the following equation:

$$LaOCl + H_2PO_4^- = LaPO_4 + H_2O + Cl^- \qquad (6)$$

At the same time, pseudomorphic transformation was observed by SEM, yielding ordered arrays of nanorods (Figure 8). The size and the alignment of nanorods were concentration-dependent and could be changed by means of surfactant adding. At high ammonium dihydrogen phosphate content (1 M and greater), we obtained aligned nanorods of 15−30 nm thickness, oriented perpendicularly to the basal planes of the original crystallites (Figure 8a). The specific surface area was increased to 45 $m^2/g$. Lower phosphate contents (0.5 M and lower) led to the formation of interconnected networks of rods (Figure 8b), with the density depending on the phosphate concentration: the higher the concentration of phosphate, the higher is the density of the rods network, and the lower their connectivity. Addition of a cetyltrimethylammonium bromide (CTAB) surfactant led to an effect similar to that of lowering of phosphate concentration, probably by retarding the propagation of the reaction front due to adsorbed CTAB species (Figure 8c). HRTEM/EDS observations confirmed that the nanorods consist of pure $LaPO_4$, with the La/P atomic ratio being equal to 1 within the accuracy limits of the EDS technique. The rods were oriented along the [100] axis of the $LaPO_4$ structure (Figure 9). The transformation from LaOCl to LaPO4 is a pseudomorphic but not topotactic reaction since the hexagonal structure of $LaPO_4$[34] does not contain any motifs common with that of tetragonal LaOCl.

As follows from the microscopy observations, the addition of ammonium phosphate leads, unlike the reaction with acid, to the propagation of the reaction along the [001] axis, perpendicularly to the basal planes of the initial LaOCl crystallites. The explanation of this striking difference can be inferred from considering the LaOCl structure and the possibilities of its reactivity. A fragment of the LaOCl structure projected along (100) or (010) is represented in Figure 10. Obviously, the crystalline planes of this structure are chemically very nonequivalent. The basal planes (001) expose the topmost chlorine ions and La atoms, and are expected to be acidic, therefore anion-exchanging in the acidic solutions. In the presence of phosphate, the rapid exchange of chloride to phosphate and $LaPO_4$ germination occurs on them, as straightforwardly demonstrated by AFM. By contrast, (100) and (010) chemically equivalent planes expose oxygen atoms covalently bonded to lanthanum, therefore being basic. Their protonation easily occurs in the acidic solutions not containing phosphate, leading to the dissolution of lanthanum cationic species and the propagation of the etching front perpendicular to the [001] axis, as described in the previous section. Curiously, not one of the LaOCl planes is reactive in the strongly basic solutions. Note that under strongly basic conditions, when the LaOCl surface is negatively charged, no reaction occurs even if phosphate anions are present. Finally, the simultaneous presence of a diluted acid and a complexing anion or a surfactant leads to an intermediate case. The reaction probably starts from the basal planes but can further propagate tangentially to the (001) direction. In agreement with this statement, we observed that the adding of CTAB to the acidic solutions (without phosphate) strongly hinders the reactivity of LaOCl.

Overall, being able to regulate the reactivity of selected crystalline planes of LaOCl, we obtain a tool for tailor-made morphology tuning of the resulting $LaPO_4$. Lanthanum phosphate (monazite) is extensively studied, mostly as a host for luminescent materials[35,36] but also in ceramics,[37,38] protonic conductors,[39] and catalysis.[40,41]

(34) Mooney, R. C. L. *Acta Crystallogr.* **1950**, *3*, 337.

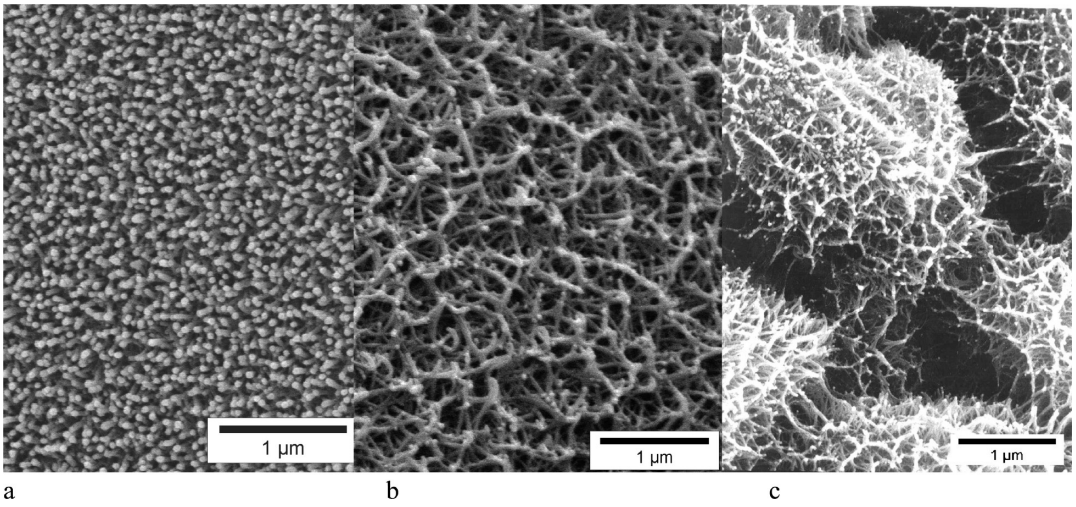


**Figure 8.** SEM images of $LaPO_4$ nanorods obtained from the interaction of LaOCl with ammonium dihydrogen phosphate for one day in 1 M solution (a); 0.01 M solution (b); and in 1 M phosphate solution the presence of 0.005 M CTBA (c).

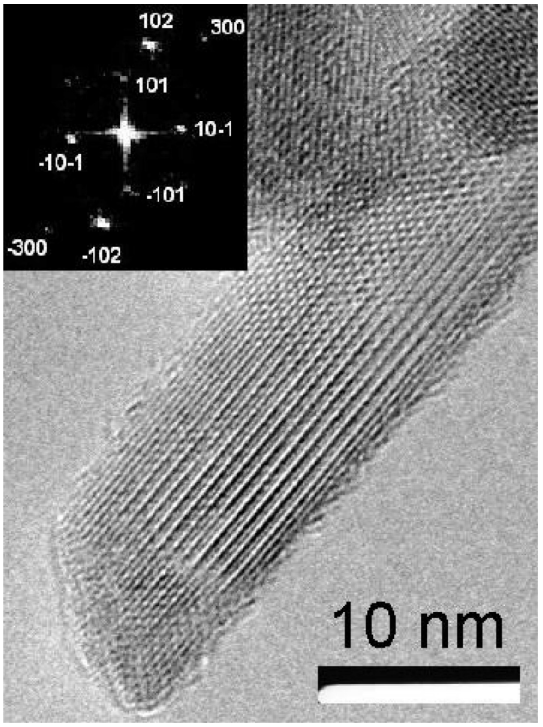


**Figure 9.** High resolution TEM image of a $LaPO_4$ nanorod.

Control of $LaPO_4$ morphology is an actively pursued challenge, addressed in several recent works.[42−44] Exemplified by the formation of $LaPO_4$ nanorods, the technique reported here is by no means limited by this particular case. Preliminary studies have shown that the LaOCl material can be transformed to a variety of products using ionic species such as vanadate or fluoride. However, a detailed description is out of scope of the present work.

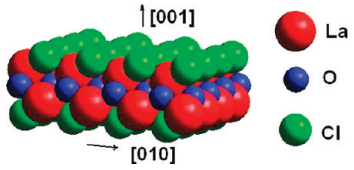


**Figure 10.** Fragment of the LaOCl crystalline structure.

**3.4. Isopropanol Decomposition Catalytic Activity.** We studied the morphology of LaOCl and the derived solids primarily with the scope of their catalytic applications. It was pointed out earlier that the acid−base properties of LaOCl are of primary importance for its catalytic performance.[45] Isopropanol (IPA) decomposition under nitrogen atmosphere was chosen to characterize the catalytic properties of our solids. The relative rates and activation energies of acetone and propene production can be used as a good qualitative estimate of the acid−base properties. DFT calculations and IR spectroscopy of adsorbed probe molecules suggested that the LaOCl possesses Lewis acid sites of strength intermediate between that of $La_2O_3$ and $LaCl_3$.[46] However, unlike these two compounds, LaOCl has a strongly anisotropic structure. Such anisotropy may lead to a striking dependence of acid−base properties on the solid morphology due to preferential exposure of the chemically very unequal crystallographic planes.

IPA conversion was studied in the temperature range 250−320 °C where the only organic products are acetone

(35) Ghosh, P.; Oliva, J.; De la Rosa, E.; Haldar, K. K.; Solis, D.; Patra, A. *J. Phys. Chem. C* **2008**, *112*, 9650.
(36) Chai, R.; Lian, H.; Yang, P.; Fan, Y.; Hou, Z.; Kang, X.; Lin, J. *J. Colloid Interface Sci.* **2009**, *336*, 46.
(37) Morgan, P. E. D.; Marshall, D. B. *J. Am. Ceram. Soc.* **1995**, *78*, 1553.
(38) Wang, R.; Pan, W.; Chen, J.; Fang, M.; Jiang, M.; Cao, Z. *Ceram. Int.* **2003**, *29*, 83.
(39) Amezawa, K.; Maekawa, H.; Tomii, Y.; Yamamoto, N. *Solid State Ionics* **2001**, *145*, 233.
(40) Onoda, H.; Taniguchi, K.; Tanaka, I. *Micr. Mesopor. Mater.* **2008**, *109*, 193.
(41) Takita, Y.; Sano, K.; Muraya, T.; Nishiguchi, H.; Kawata, N.; Ito, M.; Akbay, T.; Ishihara, T. *Appl. Catal., A* **1988**, *170*, 23.
(42) Hudry, D.; Rakhmatullin, A.; Bessada, C.; Bardez, I.; Bart, F.; Jobic, S.; Deniard, P. *Inorg. Chem.* **2009**, *48*, 7141.
(43) Hou, Z.; Wang, L.; Lian, H.; Chai, R.; Zhang, C.; Cheng, Z.; Lin, J. *J. Solid State Chem.* **2009**, *182*, 698.
(44) Bu, W.; Zhang, L.; Hua, Z.; Chen, H.; Shi, J. *Cryst. Growth Des.* **2007**, *7*, 2305.
(45) Podkolzin, S. G.; Manoilova, O. V.; Weckhuysen, B. M. *J. Phys. Chem. B* **2005**, *109*, 11634.
(46) Manoilova, O. V.; Podkolzin, S. G.; Tope, B.; Lercher, J.; Stangland, E. E.; Goupil, J. M.; Weckhuysen, B. M. *J. Phys. Chem. B* **2004**, *108*, 15570.

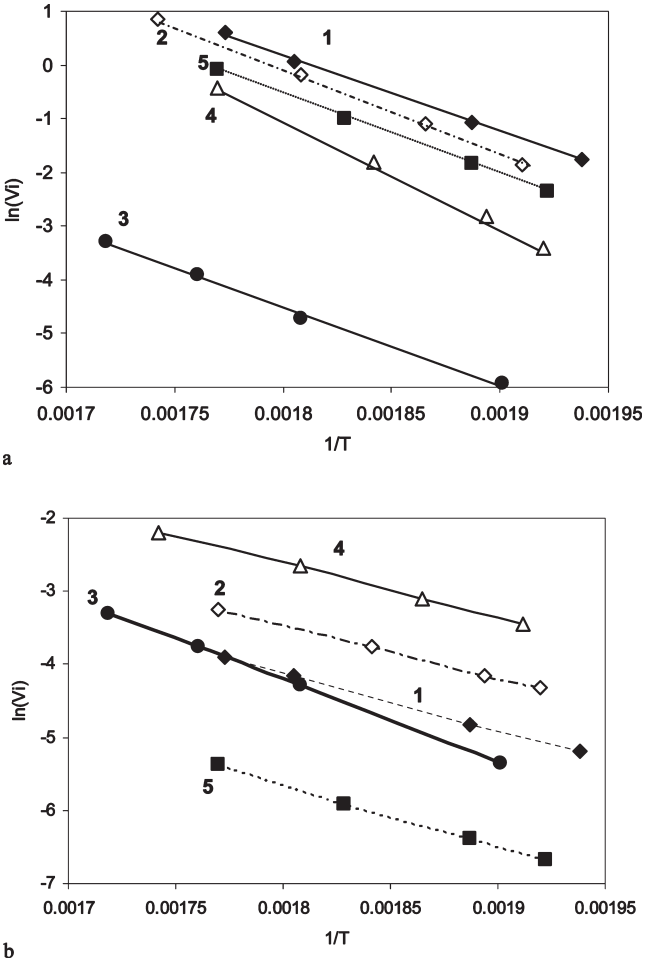


**Figure 11.** Arrhenius plots of specific rates of isopropanol conversion to propene (a) and acetone (b) in the presence of initial LaOCl and differently treated solids. Labels: 1, initial LaOCl; 2, HCl-treated LaOCl; 3, KOH-treated LaOCl; 4, $La(OH)_3$ nanofibers; 5, $LaPO_4$ nanorods.

(supposed to be produced on basic sites) and propene (acidic sites). In the last case, water is also produced. The interpretation of the intrinsic reaction rates is straightforward: the relative specific rates of the formation of two products are diagnostic. As with the activation energies, that for the propene production is usually lower for more acidic solids, and that for the acetone production usually decreases with the increase of the solids' basicity.[47]

The results of IPA decomposition tests are depicted in Figure 11 for the initial and treated LaOCl. The activities of $LaPO_4$ and $La(OH)_3$ nanorods are given for comparison and can be considered as references. Numeric values of activation energies and the rate constant ratios are summarized in Table 1. $LaPO_4$ is mildly acidic and shows almost no basicity, in agreement with earlier work,[48,49] whereas $La(OH)_3$ shows both acidic and basic functionalities with a strong prevalence of basic character, again in agreement with the previous work on its properties and on the pronounced basicity of $La_2O_3$ oxide, which is reversibly rehydrated toward $La(OH)_3$ at relatively low temperatures.[50,51] For the solid treated with KOH, the acidity dropped dramatically as compared with the initial LaOCl, but no concomitant increase of basicity was observed.

The most important finding concerns the catalysts containing the unchanged LaOCl phase. The initial LaOCl showed distinct acidic properties. After treating with HCl, the relative basicity was increased by a factor of 3. At the same time, conversion to propene slightly decreased after the same HCl treatment, which leads to a neat 4-fold $k_a/k_b$ drop. A counterintuitive relationship exists therefore in this case between the acidity of the treating solution and that of the solid product. Indeed, initial LaOCl prepared in a moderately basic nitrate melt demonstrates pronounced acidity, whereas after treatment with HCl, it becomes more basic. This effect can be tentatively explained by the change of morphology. Indeed, the acid centers of the initial LaOCl are bound to be located on the (001) planes since the proportion of other planes in this solid is negligible. The rods of the HCl-treated solid demonstrated increased basicity perhaps due to the increased exposure of oxygen-containing (100) and (010) planes. Note that surface relaxation and reorganization are possible within the same crystallographic planes due to the adsorption of reactants. However, we do not propose any detailed structural model here but only postulate the striking difference of activity between the initial LaOCl and nanorods produced from its etching. The morphology of all of the solids before and after catalytic tests was the same, and no new phases appeared after the catalytic test according to XRD and Raman studies (Figures S2 and S4, Supporting Information). At the same time, modification of the surface composition according to XPS was negligible. Neither TEM attested any variation of the nanorod's shape and composition. Therefore, the same LaOCl particles were active throughout the duration of the catalytic test. Alternatively, in the case of a strong variation of composition within the same structure, the XRD lines should be significantly broadened, the XPS composition would be modified and/or the Raman bands should be broadened and shifted, which is also not the case. No doubt that a complex evolution of surface species occurred during the reaction, but these questions are beyond the scope of this work.

Since the preparations were carried out under aerobic conditions, adsorbed carbonate is necessarily present. Carbonate vibration lines cannot be reliably seen either by IR (Figure S3, Supporting Information) or by Raman spectroscopy (Figures S4 and S5, Supporting Information). However, carbonate was detected by XPS spectroscopy as a high-energy (288 eV) component of the C1s line (Figure S6, Supporting Information). The estimated amount of carbonate was about 18% of the total carbon species or about 3−4% of the total surface composition. The amount of carbonate was similar in the samples before and after the catalytic test. Carbonate

(47) Gervasini, A.; Auroux, A. *J. Catal.* **1991**, *131*, 190.
(48) Takita, Y.; Kurosaki, K.; Ito, T.; Mizuhara, Y.; Ishihara, T. *Stud. Surf. Sci. Catal.* **1994**, *90*, 441.
(49) Rajesh, K; Shajesh, P; Seidel, O; Mukundan, P.; Warrier, K. G. K. *Adv. Funct. Mater.* **2007**, *17*, 1682.
(50) Rosynek, M. R.; Magnuson, D. T. *J. Catal.* **1977**, *46*, 402.
(51) Corma, A.; Iborra, S. *Adv. Catal.* **2006**, *49*, 239.

**Table 1. Arrhenius Parameters of the IPA Conversion Rate to Propene and Acetone**

| solid | Ea propene (kJ/mol) | $A_{propene}$[a] | Ea acetone (kJ/mol) | $A_{acetone}$ | $k_a/k_b$[b] |
|---|---|---|---|---|---|
| LaOCl initial | 118 ± 7 | 25 | 69 ± 4 | 9 | 1 |
| LaOCl − 0.1 M HCl | 112 ± 5 | 23 | 63 ± 4 | 10 | 0.25 |
| LaOCl − 0.1 M KOH | 120 ± 10 | 20 | 96 ± 6 | 16 | 0.0006 |
| $La(OH)_3$ | 164 ± 8 | 26 | 60 ± 4 | 11 | 0.0045 |
| $LaPO_4$ | 123 ± 6 | 33 | 72 ± 5 | 9 | 1.8 |

[a] Pre-exponential factor, $\mu mol/m^2 \cdot s$, ±1. [b] Relative acidity, expressed as the rate constant ratio for acetone and propene at 275 °C, normalized to the initial LaOCl.

species are reversibly formed on the surface of LaOCl, which is the basis of their use as sensors (refs 19 and 21). In our case, carbonate does not seem to be accumulated at the surface during a catalytic test and/or to play any determining role for the variations of catalytic activity between differently treated solids.

In the Raman spectra of LaOCl etched with HCl (before or after the test), we see only the lines of pure LaOCl (Figure S5, Supporting Information). This is a seeming contradiction with the results of ref 18, where treatment with HCl led to appearance of intense $LaCl_3$ lines. This is explained by the difference in conditions. While in ref 18 the treatment of LaOCl with HCl was carried out in the gas phase and $LaCl_3$ was accumulated in the solids, in our case, since HCl treatment was carried out in the solution, water-soluble $LaCl_3$, once formed, was immediately removed from the solid.

It was observed earlier that LaOCl catalysts can be transformed to other phases under reaction conditions. Thus, $LaCl_3$ and $La_2O_3$ can be formed in a dynamic equilibrium in LaOCl during the destruction of $CCl_4$ by water vapor.[52] In our case, the evolution of the catalysts after the IPA decomposition test was negligible since the water vapor partial pressure was 2 orders of magnitude lower than that used in ref 52. The XPS-derived La to Cl ratio remains the same within the accuracy limits of this method (Table S2, Supporting Information). Raman spectra of the catalysts measured before and after the IPA decomposition test show the same six lines characteristics for LaOCl vibration modes as described in ref 53 (Figure S4, Supporting Information). Furthermore, the TEM study of all used catalysts shows that the morphology remains essentially the same before and after catalytic tests (usually 36 h), which of course does not exclude some evolution of the surface composition.

(52) Van der Avert, P.; Podkolzin, S. G.; Manoilova, O. V.; De Winne, H.; Weckhuysen, B. M. *Chem.—Eur. J.* **2004**, *10*, 1.
(53) Hölsä, J.; Koski, K.; Makkonen, S.; Säilynoja, E.; Rahiala, H. *J. Alloys Compd.* **1997**, *249*, 217.

## 4. Conclusions

As exemplified by the LaOCl case, ordered arrays of uniformly sized nanororods can be obtained by pseudomorphic solid−liquid reactions of an appropriate crystalline precursor, in a controllable manner. Such a control can be achieved both for metathesis or etching reactions, on a common basis of different reactivity of the precursor solid planes toward the solution. By means of using surfactants or complexing anions of varying content, the morphology of the products can be finely tuned. The resulting materials, while remaining the same LaOCl compound, have strongly different catalytic properties as demonstrated in the example of acid−base properties of differently oriented LaOCl. This approach can be extended to other types of solids and particularly those which have a strong structural anisotropy. We are striving to extend this method to compounds such as lamellar hydroxides or sulphides. A crucial point to extend this strategy is the preparation of well crystallized and oriented initial solids, which would be further transformed to the ordered arrays of the products.

**Supporting Information Available:** The results of elemental and EDS analysis; quantitative XPS of selected samples before and after catalytic tests; XRD, IR and Raman spectra of selected samples before and after catalytic test (PDF). This information is available free of charge via the Internet at http://pubs.acs.org/.